Alma Mater Studiorum Università di Bologna
Archivio istituzionale della ricerca

Structure and dynamics of methacrylamide, a computational and free-jet rotational spectroscopic study

(Article begins on next page)

05 May 2024

Structure and dynamics of methacrylamide,
a computational and free-jet rotational spectroscopic study.

A. Maris, S. Melandri, L. Evangelisti, A. Vigorito, S. Sigismondi, C. Calabrese, I. Usabiaga.

Structure and dynamics of methacrylamide, a computational and free-jet rotational spectroscopic study

Assimo Maris [a,*], Sonia Melandri [a], Luca Evangelisti [a], Annalisa Vigorito [a], Silvia Sigismondi [a],
Camilla Calabrese [b,c,d], Imanol Usabiaga [b,c]

[a] *Dipartimento di Chimica "G. Ciamician", Università di Bologna, via Selmi 2, I-40126 Bologna, Italy*
[b] *Departamento de Química Física, Universidad del País Vasco (UPV/EHU), Apartado 644, E-48080 Bilbao, Spain*
[c] *Biofisika Institute (CSIC, UPV/EHU), Barrio Sarriena, S/N, E-48940, Spain*
[d] *Fundación Biofisika Bizkaia/Biofisika Bizkaia Fundazioa (FBB), Barrio Sarriena, S/N, E-48940, Spain*

ABSTRACT

The conformational space of methacrylamide was explored by quantum mechanical modeling and surveyed in the 59.6–104.0 GHz frequency range using a millimeter-wave Stark-modulated free-jet absorption spectrometer. According to the relative orientation of the two unsaturated bonds, two conformers were observed, namely s-*trans* (A=5234.360(1), B=3364.9717(8) and C=2173.099(1) MHz) and s-*cis* (A=5207.292(1), B=3470.930(1) and C=2113.496(1) MHz). The s-*trans* conformation is the global minimum, with relative energy 4(2) kJ mol^{-1} and calculated isomerization barrier 15 kJ mol^{-1}. Except for the methyl hydrogen atoms, s-*cis*-methacrylamide is planar and its methyl internal rotation barrier is 10.2(1) kJ mol^{-1}. In s-*trans*-methacrylamide the allyl and amino frames form a dihedral angle of about 30° and the methyl internal rotation barrier is 7.4 kJ mol^{-1}. This different behaviour is explained in terms of attractive and repulsive intramolecular interactions between groups: CH_2/CO and CH_3/NH_2 for s-*cis*, CH_2/NH_2 and CH_3/CO for s-*trans*. The tunneling splitting related to the double-well potential describing the interconversion between the two equivalent s-*trans* forms is 837.97(2) MHz and was reproduced by a one-dimensional flexible model using a 3.6 kJ mol^{-1} interconversion barrier.

Introduction

The structure and the charge distribution define the properties of a molecule. For instance in the lock-and-key mechanism proposed in 1890 by Emil Fischer, a ligand (the key) can bind the receptor only if its structure matches the active site shape (the lock). However, the interaction is bidirectional and as a molecule acts on the surrounding environment so the environment influences the shape of the molecule. Indeed, molecules are not rigid bodies, but adaptable objects whose structure is determined by a balance of both intra- and inter-molecular non covalent interactions. Among many examples, well known cases are the folding of proteins and the double helix structure of nucleic acids. In particular the flexibility of a molecule increases with the number of rotatable bonds, generating an increasing number of possible stable structures called conformers. The full exploration of the structural space can be approached only for the smallest systems, whereas, more generally, efforts are devoted to the determination of local minima and the pathways connecting them, using both experimental and computational methods.

Among experimental techniques, rotational spectroscopy provides structural descriptors for relatively small molecules in isolated phase. This limits the size of detectable systems, but the obtained information is extremely accurate and can be directly used for spectral identification of molecules in radio astronomical sources [1]. Moreover, in an isolated environment, large amplitude motions can greatly affect the rotational spectral shape, allowing to achieve data on the corresponding shallow minimum regions of the structural space, the reliable prediction of which constitutes an issue for theoretical simulations.

In our group, we have been investigating since a long time the structural and dynamical behaviour of amides variously substituted in relation to their relevance in biological issues [2–10]. They give rise to the peptide linkage between two amino acids in proteins and are also commonly found in drugs such as the β-lactam antibiotic family [11], anesthetics [12] and antipyretics [13]. The presence of the N-H and C=O dipoles allows for amide frames to act as hydrogen bond donors and acceptors giving place to two main kind of secondary structures in proteins: α-helix [14] and β-sheet

---

* Corresponding author.
   E-mail address: assimo.maris@unibo.it (A. Maris).
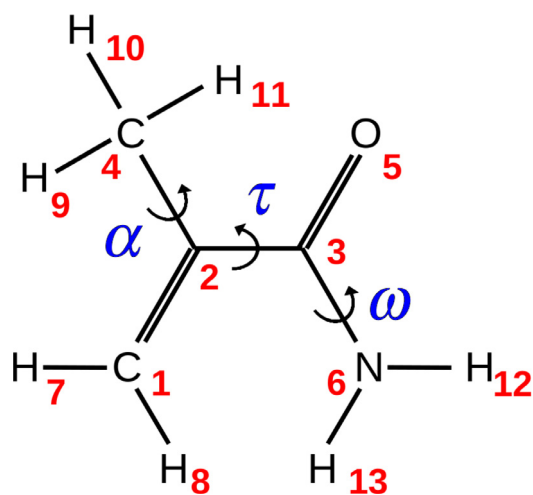
Fig. 1. Sketch, atoms' numbering, and torsional coordinates of methacrylamide.

Fig. 2. Theoretical potential energy for the skeletal torsion of methacrylamide, $E(\tau)$.

[15]. Furthermore, amides' poor reactivity and stability at physiologic pH allow for keeping the protein primary structure and thus their functions unchanged. Unlike amines, amides behave neither as bases nor as nucleophiles due to the fact that the electronic lone pair on the nitrogen atom is delocalized on the adjacent carbonyl group forming a N-C partial double bond. This delocalization also reduces the electrophilic nature of the carbonyl present in amides relative to that of the carbonyl groups in compounds such as aldehydes and ketones. In this paper, we present a conformational study of methacrylamide performed with quantum mechanical calculations and free-jet rotational spectroscopy. From a spectroscopic point of view, the study of methacrylamide is challenging. Even though it has only six heavy atoms (Fig. 1), because of the proximity of four interacting functional groups a complex internal dynamics, involving the torsion around the C2-C3 single bond connecting the allyl non polar frame and the amide polar frame, the methyl internal rotation and the wagging of the amino group could be found. To our knowledge, no previous rotational spectroscopy data on methacrylamide are available, whereas a theoretical investigation on the torsional pathways has already been performed using B3LYP and MP2 methods coupled to Pople's split valence triple-ζ basis sets, together with the analysis of the vibrational normal modes obtained at the B3LYP/6-311+G(d,p) level of calculation [16].

Computational details

Quantum mechanical calculations, aimed to explore the structural space and to characterize the stationary points (local minima and transition states), were performed employing the GAUSSIAN16[TM][1] software package (G16, Rev. A.03). The valence triple-zeta quality Dunning correlation consistent polarized type basis set augmented with diffuse functions (aug-cc-pVTZ [17]) was used in combination with three methods: the Møller-Plesset second order perturbation theory (MP2 [18]) and the Becke-three-parameters Lee-Yang-Parr hybrid density functional theory (B3LYP [19,20]), both in the original version and corrected by the D3BJ [21] Grimme empirical dispersion (B3LYP-D3). Evaluation of harmonic force field was pursued with all the mentioned methods, whereas anharmonic corrections were included through the second
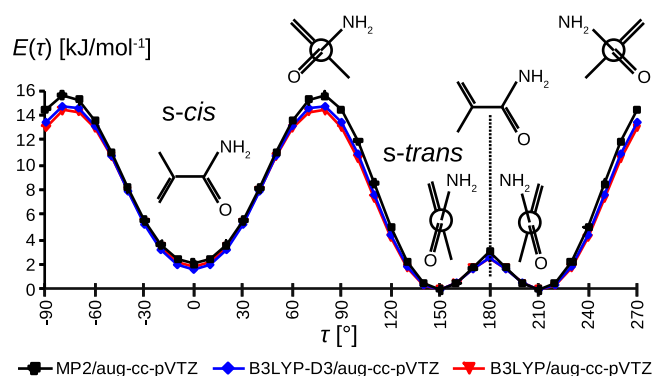
order vibrational perturbation theory [22] only at the B3LYP/aug-cc-pVTZ level of calculation. Torsional energy pathways were calculated varying the corresponding coordinate by steps of 10°, while all the other parameters were freely optimized. The C2-C3 torsional path, obtained at the B3LYP-D3/aug-cc-pVTZ level of calculation was directly analyzed by an automatised flexible model [23] in order to determine the energies of the related vibrational modes.

Experimental details

Methacrylamide (purity 98%, molecular weight 85.11 g mol^{-1}) was purchased from Alfa-Aesar and used without any further purification. It appears as white odorless crystals, with melting point 380–385 K (107–112 °C) and boiling point 488 K (215 °C). Argon, purchased from SIAD (Società Italiana Acetilene e Derivati), was used as carrier gas. The rotational spectrum was recorded in the millimeter-wave region (5.03-2.72 mm, 59.6–104.0 GHz) using a Stark-modulated free-jet absorption spectrometer [3,24,25]. The estimated uncertainties for the measurements is about 50 kHz. The sample was heated to 353 K (80 °C) while a stream of argon (P_0=18 kPa) was flowed over it. The mixture was then expanded to about P_b=0.5 Pa through a 0.3 mm diameter pinhole nozzle heated to T=363 K (90 °C). The estimated rotational temperature of the molecules in the jet is about 5–10 K. This value has been estimated from relative intensity measurements on Q-branch bands observed in previously studied molecular systems, such as 1,2-butanediol [25] and 1-chlorobutane [26].

Exploring the structural space

Methacrylamide is formed by an allyl and an amide frames connected by a rotatable bond. Both frames, as a first approximation, have a C_s symmetry and their relative orientation, described by the C1=C2-C3=O5 dihedral angle (τ), defines the structure of the molecule. An energy scan along this torsional coordinate provides the potential energy surface, $E(\tau)$, given in Fig. 2. There are two low energy regions, one at τ=0°, corresponding to a s-cis orientation of the two unsaturated bonds, and the other at around τ=180°, corresponding to a s-trans arrangement. In the s-trans region, $E(\tau)$ has a double-minimum shape in which the minima, lying at $\tau \approx 150°$, are separated by a barrier of 2.5-3 kJ mol^{-1}, corresponding to a planar skeletal structure. These minima are enantiomers and, due to the low value of the energy barrier, constitute a transient chirality system. Conversely, the s-cis region is characterized by a single minimum, which is less stable than the s-trans one by about 2 kJ mol^{-1}, and corresponds to a C_s symmetry structure in which only the methyl hydrogen atoms lie out of
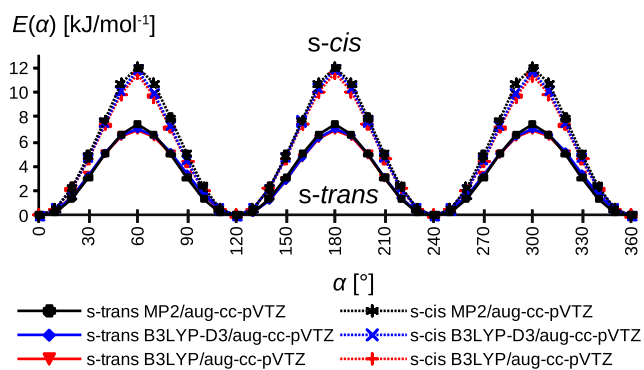
Fig. 3. Theoretical potential energy for the methyl internal rotation of s-*trans*- and s-*cis*-methacrylamide, $E(\alpha)$.

Fig. 4. Excerpt of the free-jet absorption spectrum of methacrylamide showing the $8_{6,2}$-$7_{5,3}$ transition line of both s-*trans*- and s-*cis*-methacrylamide, which are depicted with their principal inertial axes at the top.

Fig. 5. Excerpt of the free-jet absorption spectrum of s-*trans*-methacrylamide showing the $7_{3,4}$-$6_{2,5}$ transition line with the assignment of the hyperfine structure arising from the inversion motion ($0^+/0^-$ states), the ^{14}N quadrupole coupling interaction (F quantum numbers), and the methyl internal rotation (A/E states).

the symmetry plane. $E(\tau)$ shows two equivalent absolute maxima corresponding to a s-*trans* to s-*cis* isomerization barrier of about 15 kJ mol^{-1}. In the corresponding two transition states the allyl and amide frames are almost perpendicular to each other (τ=80°). It is worth noting that the skeletal torsion motion is coupled to the wagging motion of the amino group (ω).

Comparing our data with those obtained using Pople's basis sets [16], we find that the predicted energy difference between conformers is more sensitive to the basis set in the case of MP2 (6-311G(d,p) 4.7, 6–311+G(d,p) 5.6, aug-cc-pVTZ 2.1 kJ mol^{-1}) instead of B3LYP (6-311G(d,p) 1.3, 6–311+G(d,p) 1.5, aug-cc-pVTZ 1.8 kJ mol^{-1}). However, we also observe that comparing the results obtained with the same basis set, the smallest difference between the MP2 and B3LYP values is obtained using aug-cc-pVTZ.

The G16 output file concerning the torsional path obtained at the B3LYP/aug-cc-pVTZ level of calculation was directly used as input of an automatised flexible model [23], which provided the vibrational eigenvalues and eigenstates related to the torsion motion. As regards the s-*trans* species, we find that the ground vibrational state (ν=0) lies below the interconversion barrier and, due to quantum tunnelling, it is split into two states separated by 3.3 GHz. These states are symmetric (ν=0$^+$) or antisymmetric (ν=0$^-$) with respect to the torsional coordinate, which in this region can be considered as an inversion coordinate occurring parallel to the molecular c-axis.

Besides the skeletal torsion coordinate, also the methyl internal rotation, represented by the H9-C4-C2-C1 dihedral angle (α), must be considered. The related calculated potential energy paths, $E(\alpha)$, for the two conformers are depicted in Fig. 3. A threefold shape path is found for both forms. For the s-*trans* form the barrier is about 7 kJ mol^{-1}, corresponding to a predicted splitting between the A and E states of about 40 MHz. The barrier is higher in the s-*cis* conformer, about 12 kJ mol^{-1}, leading to smaller A/E splitting, about 1 MHz.

Rotational spectrum

The free-jet rotational spectrum of methacrylamide, recorded in the 59.6–104 GHz frequency region, was analyzed with the CALPGM program suite [27], using the Watson S-reduction and I^r representation [28]. Preliminary predictions were done on the basis of the theoretical spectroscopic parameters reported in Table 1. Strong μ_b-type and weak μ_a-type transition lines belonging to both conformers were easily assigned. Looking at the spectrum reported in Fig. 4, one can compare the $8_{6,2} - 7_{5,3}$ transition line detected for both conformers at about 72 GHz. Two main findings
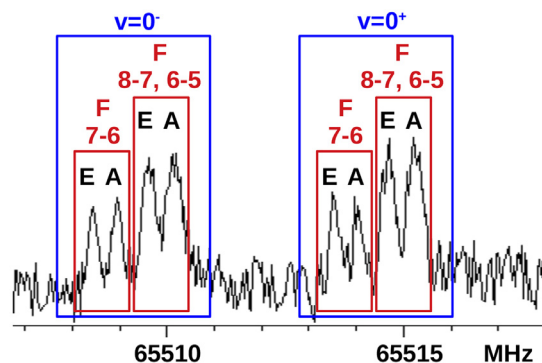
emerge: (*i*) the s-*cis* line is weaker than the s-*trans* one, despite its μ_b electric dipole moment being bigger, thus the s-*trans* species is the global minimum, with an estimated energy difference 4(2) kJ mol^{-1}; (*ii*) the s-*trans* line is split, in agreement with the presence of two inversion tunnelling states. The latter consideration is confirmed by the observation of several μ_c-type interstate transition lines, in agreement with the inversion of the μ_c electric dipole moment component between the two equivalent s-*trans* structures. Moreover, as exemplified in Fig. 5, several lines showed additional splittings due to the methyl internal rotation and the ^{14}N nuclear quadrupole interaction.

The 457 measured frequencies lines of s-*trans*-methacrylamide are listed in the Appendix (Table A1) and were assigned using the following Hamiltonian:

$$H = H_R + H_{CD} + H_Q + H_E + H_{0\pm} \tag{1}$$

where a specific rotational rigid operator is used for each of the four involved states:

$$H_R = H_R^{A,0^+} + H_R^{A,0^-} + H_R^{E,0^+} + H_R^{E,0^-} \tag{2}$$

while the quartic centrifugal distortion operator (H_{CD}) is common to all states. Two different operators associated with the quadrupo-

Table 1
Theoretical molecular descriptors of methacrylamide calculated with the aug-cc-pVTZ basis set.

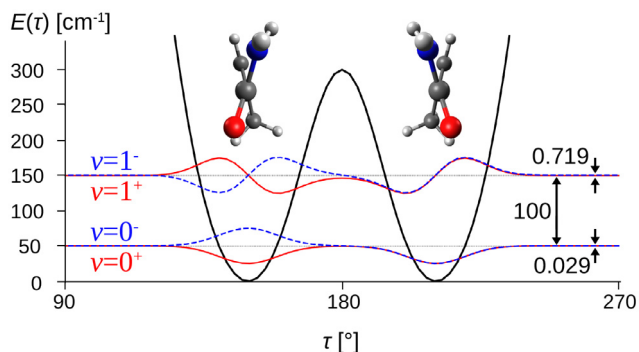|	s-*trans*-methacrylamide			s-*cis*-methacrylamide		
	MP2	B3LYP	B3LYP-D3	MP2	B3LYP	B3LYP-D3
Energy values						
E_e [hartree]	-286.083427	-286.732208	-286.749467	-286.082621	-286.731504	-286.748852
E_0 [hartree]	-285.975613	-286.625413	-286.642565	n.a.[a]	-286.624724	-286.641965
ΔE_e [kJ mol^{-1}]	0	0	0	2.12	1.85	1.63
ΔE_0 [kJ mol^{-1}]	0	0	0	n.a.[a]	1.81	1.57
Dihedral angles						
τ [°]	±149.7	±148.3	± 148.5	0	0	0
ω [°]	∓ 152.3	∓ 160.5	∓ 160.3	180	180	180
Electric dipole moment components						
μ_a [D]	-0.76	-0.74	-0.74	-1.84	-1.89	-1.89
μ_b [D]	-2.95	-3.09	-3.09	3.37	3.42	3.42
μ_c [D]	1.39	1.33	1.33	0	0	0
μ_{tot} [D]	3.35	3.45	3.45	3.84	3.91	3.91
Rotational constants						
A [MHz]	5231.565	5257.551	5259.894	5221.136	5238.441	5241.372
B [MHz]	3390.232	3350.804	3364.710	3501.649	3472.164	3484.959
C [MHz]	2188.041	2185.222	2189.888	2123.647	2115.521	2120.748
$\kappa = \frac{2B-A-C}{A-C}$	-0.210	-0.241	-0.235	-0.110	-0.131	-0.126
^{14}N quadrupole coupling constants						
χ_{aa} [MHz]	0.85	1.05	1.06	1.96	2.12	2.12
χ_{bb} [MHz]	1.90	2.10	2.09	1.83	2.01	2.01
χ_{cc} [MHz]	-2.75	-3.15	-3.15	-3.80	-4.13	-4.12
Planar moments of inertia						
M_{aa} [u Å^2]	141.72	142.99	142.45	142.75	143.98	143.45
M_{bb} [u Å^2]	89.25	88.29	88.33	95.22	94.91	94.85
M_{cc} [u Å^2]	7.35	7.84	7.75	1.57	1.57	1.57
Methyl internal rotation parameters						
$\widehat{ia}$ [°]	54.4	54.5	54.5	56.7	56.8	57.0
$\widehat{ib}$ [°]	37.6	37.8	37.7	33.3	33.2	33.0
$\widehat{ic}$ [°]	79.3	78.9	78.8	90.0	90.0	90.0
I_α [uÅ^2]	3.15	3.14	3.14	3.13	3.13	3.13
F_0 [GHz]	160.5	160.8	160.7	161.4	161.7	161.7
V_3 [kJ mol^{-1}]	7.43	6.95	6.92	12.47	11.60	12.87
Δ_0 [MHz]	31.8	46.2	46.2	0.8	1.6	0.6
D_a [MHz]	0.75	1.10	1.10	0.016	0.029	0.013

[a] Not available: the frequency of the NH$_2$ wagging mode is imaginary.

Table 2
Spectroscopic parameters of s-*trans*-methacrylamide determined from experimental frequencies' fitting, using SPFIT [27] and adopting Watson's *S*-reduction and *I*^{r}-representation. Two set of data are presented, obtained using the G_a (Fit I) or F_{bc} (Fit II) coupling constants, respectively.

	Fit I			Fit II	
	A-state	E-state		A-state	E-state
A^+ [MHz]	5234.360(1)[a]	5234.334(1)		5234.338(1)	5234.312(1)
A^- [MHz]	5234.257(1)	5234.232(1)		5234.279(1)	5234.254(1)
B^+ [MHz]	3364.9717(8)	3364.9530(8)		3364.9403(8)	3364.9216(8)
B^- [MHz]	3364.8274(8)	3364.8084(8)		3364.7960(8)	3364.7771(8)
C^+ [MHz]	2173.099(1)	2173.101(1)		2173.130(1)	2173.132(1)
C^- [MHz]	2173.186(1)	2173.188(1)		2173.217(1)	2173.220(1)
χ_{aa} [MHz]	0.47(23)	1.77(27)		0.48(23)	1.77(27)
$\chi_{bb} - \chi_{cc}$ [MHz]	4.24(6)	4.11(7)		4.24(6)	4.11(7)
D_a [MHz]	-	0.730(2)		-	0.730(2)
D_J [kHz]		0.701(2)			0.701(2)
D_{JK} [kHz]		0.15(1)			0.15(1)
D_K [kHz]		0.51(1)			0.51(1)
d_1 [kHz]		−0.297(1)			−0.297(1)
d_2 [kHz]		−0.1761(4)			−0.1762(4)
$\Delta E_{0^\pm}$ [MHz]		837.97(2)			837.97(2)
G_a [MHz]		4.278(8)	F_{bc} [MHz]		6.12(1)
σ [b] [MHz]		0.044			0.044
N [c]		457			457

[a] Standard error in parentheses in the units of the last digit. [b] Root mean square deviation of the fit. [c] Number of transitions in the fit.

Fig. 6. Potential energy and vibrational eigenfunctions for the inversion motion of s-*trans*-methacrylamide.

lar interaction of the ^{14}N nucleus with the overall rotation were considered for the A and E methyl internal rotation states, but common to the $v=0^+$ and $v=0^-$ inversion states:

$$H_Q = H_Q^A + H_Q^E \tag{3}$$

The methyl internal rotation operator, derived from a perturbation treatment of internal rotation [29] on the basis of the principal axis method (PAM [30]), acting only on the E states is:

$$H_E = D_a \cdot P_a \tag{4}$$

and the inversion operator based on the inertial axis system is:

$$H_{0\pm} = \Delta E_{0\pm} + G_a \cdot P_a \tag{5}$$

In Eqs. (4)-(5), P_a is the angular momentum operator, D_a is the torsion-rotation parameter acting on the E states, G_a is the Coriolis coupling constant between the vibrational inversion states and $\Delta E_{0\pm}$ is the energy difference between the same states. The obtained spectroscopic constants are reported in Table 2. In the same table, we show that similar results are obtained using an alternative coupling scheme based on the reduced axis system, that is defining the inversion operator as:

$$H_{0\pm} = \Delta E_{0\pm} + F_{bc} \cdot (P_b \cdot P_c + P_c \cdot P_b) \tag{6}$$

For the treatment of tunneling between two equivalent minima, the reduced axis method (RAM, Eq. (6)) is expected to be more accurate than the inertial axis method (IAM, Eq. (5)) [31], but, if there is a third minimum close in energy (the s-*cis* conformer in the present case), it may be necessary to include parameters of odd order (i.e. G_a) into the Hamiltonian to describe the tunneling between the equivalent states [32]. If the third minimum is sufficiently higher in energy, the RAM interaction Hamiltonian with even order parameters, such as F_{bc}, may be replaced by an IAM interaction Hamiltonian with odd order parameters, such as G_a [33]. This seems to be the case of methacrylamide, for which we obtain two equivalent fittings: fit I and fit II in Table 2) Indeed the rotational constants values shift by 0.02÷0.03 MHz, whereas all the other parameters remain unchanged, including the standard deviation of the fit. Despite only μ_a- and μ_b-type lines are allowed for intrastate transitions, E-type transition lines with low K_c showed additional components with respect to the expected doublets of lines, because of the presence of the "electric dipole forbidden transitions" which apparently follow μ_c-type selection rules [34].

The 134 measured frequencies lines of s-*cis*-methacrylamide are listed in the Appendix (Table A2). Among them, only 6 E-type low K_c μ_c-forbidden transition lines were observed. The overall set of detected lines was assigned through direct diagonalization of the following Hamiltonian:

$$H = H_R + H_{CD} + H_Q + H_E \tag{7}$$

where unique rigid rotor (H_R), quartic centrifugal (H_{CD}) and nuclear quadrupole interaction (H_Q) operators were used for the A and E states, and H_E is the same perturbation term as for Eq. (4). Since the s-*cis* conformer is not affected by Coriolis' perturbation, besides the Hamiltonian implemented in the CALPGM program suite, we could also apply the combined axis method (CAM [35]) implemented in the XIAM program [36], which fits a common set of rotational constants for both the A and E states and directly supplies the methyl internal rotation barrier. The values of the angles between the internal rotation axis (i) and the principal inertial axes (a, b and c), and the moment of inertia of the internal top (I_α) were fixed to the MP2/aug-cc-pVTZ values (Table 1). The spectroscopic constants obtained with the two methods, are compared in Table 3.

Discussion

Structure

Planar moments of inertia describe the displacement of the masses (m_i) along the principal inertial axes:

$$M_{gg} = \Sigma_i m_i \cdot g_i^2 \qquad g = a, b, c \tag{8}$$

They are related to the rotational constants and can be obtained by linear combination of the moment of inertia, for instance M_{cc} is given by:

$$M_{cc} = \frac{I_{aa} + I_{bb} - I_{cc}}{2} \tag{9}$$

For planar molecules, with atoms lying on the ab inertial plane, the M_{cc} value is expected to be zero, and slightly positive and negative values are explained in terms of out of plane and in plane large amplitude motions, respectively [37]. In the case of molecules with C_s symmetry, and only out of plane methyl hydrogen atoms, a contribution around 1.57 u Å^2 is expected for each methyl group. This is exactly the case of s-*cis*-methacrylamide, for which M_{cc}=1.57 u Å^2 is predicted by rigid calculations (Table 1) and M_{cc}=1.79 u Å^2 is obtained when including vibro-rotational coupling by anharmonic vibrational B3LYP/aug-cc-pVTZ calculations, perfectly matching the

M_{cc}=1.77 u Å^2 experimental value. Vibro-rotational analysis shows that the vibrational motions that most affect the M_{cc} value are the CCC in plane bendings and the out of plane torsion between the amide and allyl groups (τ) and the wagging of the amino group (ω). The C_s symmetry of this conformer is also confirmed by the fact that, except for six μ_c-type forbidden E transition lines, only μ_a-type and μ_b-type transition lines were observed, in agreement with a null value of the μ_c electric dipole moment component. We note that at the MP2/aug-cc-pVTZ level of calculation, despite full and free geometry optimization leads to a C_s arrangement, an imaginary vibrational frequency is obtained involving a combined motion between the amino wagging (ω) and the methyl internal rotation (α). This unusual behaviour can be explained thinking to the HNCCCH frame as a ring closed by a H-H link, where a pseudorotation motion allows to switch between conformers avoiding the C_s arrangement, but the underlying potential energy surface is so shallow that the minimisation process converges in any case to the C_s arrangement. In this hypothesis, the vibrational ground state lies above the local maximum energy point and an effective C_s structure is observed. The planar or pyramidal structure of the amino group in isolated amide compounds is a long time debated topic. As regards the simplest amide (formamide), based on the observation of an unusually intense signal related to the NH$_2$ wagging vibrational satellite, Costain and Dowling proposed a pyramidal model and an inversion barrier of 370±50 cm^{-1} [38], while Hirota *et al.* determined a single-minimum anharmonic inversion potential, $V(\omega) = V_2 \cdot \omega^2 + V_4 \cdot \omega^4$ [39]. Nowadays, the planar structure of formamide is agreed upon [40]. However other amide compounds seem to have a double-minimum amino inversion potential with a very small inversion barrier, which allows for an effectively planar ground-state arrangement [40].

As regards s-*trans*-methacrylamide, the experimental value of the planar moment of inertia along the *c* axis, M_{cc}=7.09 u Å^2, clearly indicates that the structure is skewed, although its value is slightly smaller than those calculated in the rigid approximation (Table 1). The inversion splitting associated with the interconversion motion between the two equivalent skewed forms is 0.83797(2) GHz, about ¼ of the predicted value. This means that the inversion barrier should be higher than the calculated one, indeed, using the automatized flexible model [23], we could reproduce the experimental value scaling the torsional energy function using a factor 1.459, and obtaining an inversion barrier equal to 3.6 kJ mol^{-1} (Fig. 6). In the crystal structure the heavy atom structure of s-*trans*-methacrylamide is closer to being planar than in the gas phase, being $\tau \approx 170°$ [41] instead of $\tau \approx 150°$. In detail, methacrylamide crystallizes as conformational polymorphs, where each amide group establishes four OH·N hydrogen bonds. The orthorhombic, space group *Pabc* form contains the s-*trans* conformer and the torsional angle is τ=173.5° at 294 °C and τ=171.5° at 120 °C. The monoclinic, space group $P2_1/n$ form contains the s-*cis* conformer and the torsional angle is close to zero (τ=1.9°= at 294 °C, and τ=5.8° at 120 °C). The theoretical bond distances for the isolated conformers and the experimental solid state bond distances determined from the Crystallographic Information File given in [41] are listed in the Appendix (Figs. A1 and A2).

Methyl internal rotation

Looking at the methyl internal rotation, the experimental torsion-rotation parameter of s-*trans* conformer (D_a=730(2) kHz) is an order of magnitude greater than the s-*cis* one (D_a=77(5) kHz). These values can be combined with structural parameters to evaluate the dimensionless perturbation first-order coefficients for the

Table 4
Methyl internal rotation barrier in allyl compounds, V_3 [kJ mol^{-1}].

	s-*trans*	s-*cis*
Methacrolein [47]	5.8792(3)	n.a.
Methacrolein (IR) [46]	5.31(4)	5.27(2)
Methacryloyl fluoride [48]	7.1	n.a.
Methacrylic acid [45]	7.31(1)	9.30(2)
Methacrylamide	7.4	10.2(1)
Propene [39]	8.3529(6)	

Table 5
Experimental ^{14}N nuclear quadrupole coupling constants of methacrylamide, χ_{gg} [MHz].

	χ_{aa}	χ_{bb}	χ_{cc}
s-*trans* A	0.47(23)	1.88(15)	-2.36(15)
s-*trans* E	1.77(27)	1.17(17)	-2.94(17)
s-*cis*	1.88(9)	1.86(9)	-3.75(9)

threefold barrier introduced by Herschbach [42]:

$$W_{0,E}^{(1)} = \frac{D_a}{A \cdot \cos(\widehat{ia})} \tag{10}$$

The obtained coefficients can then be related to the reduced barrier (*s*) by tabulated data [43], allowing the estimation of the methyl internal rotation barrier as:

$$V_3 = \frac{9}{4} \cdot \frac{F_0 \cdot s}{r} \tag{11}$$

where F_0 is the rotational constant for the rotation of the methyl top around its C_3 axis and *r* is an adimensional reducing factor related to the molecular structure [44]. Moreover, using tabulated data [42], it is possible to evaluate the Fourier coefficients of Mathieu's eigenvalues for the ground state ($w_1^{v=0}$) and thus to calculate the splitting between the A and E levels as follow:

$$\Delta_0 = \frac{27}{8} \cdot \frac{F_0}{r \cdot w_1^{v=0}} \tag{12}$$

The resulting estimations are V_3=7.4 kJ mol^{-1} and Δ_0=32 MHz for s-*trans*-methacrylamide and V_3=10.2 kJ mol^{-1} and Δ_0=4 MHz for s-*cis*-methacrylamide. For the latter conformer, the value of methyl internal rotation barrier directly fitted using the XIAM program [36] is the same as expected: 10.2(1) kJ mol^{-1}. Even if the atoms connectivity does not change, the methyl rotation is more hindered by the proximity of the amino group with respect to that of the carbonyl. The same trend is found in the case of methacrylic acid [45], but not for methacrolein [46], as it can seen in Table 4, where the V_3 values of some allyl compounds are compared.

Nuclear quadrupole coupling interaction

The ^{14}N quadrupole coupling constants in the principal axes systems are given in Table 5 for both conformers. A good agreement between experimental and calculated data is found for the s-*cis* conformer, the MP2 values being closer to the B3LYP ones. Moreover, the out of plane component (χ_{cc}=-3.75(9) MHz) is comparable to those of other C_s amides like formamide (-3.835(5) MHz [49]), acetamide (-3.945(2) MHz [50]), propiolamide (-3.908(3) MHz [51]), and thioacetamide (3.66(10) MHz [3]).

Table 6

Relative conformational stability of acrolein and methacrolein compounds, $\Delta E = E_{s-cis} - E_{s-trans}$ [kJ mol^{-1}].

	R=H	R=CH$_3$
CH$_2$=C(R)-CO-HCH$_2$=C(R)–CO–H	7.9(5) [52]	9.1(4) [46]
CH$_2$=C(R)-CO-FCH$_2$=C(R)–CO–F	0.4(4) [53]	4.3(1) [54]
CH$_2$=C(R)-CO-OHCH$_2$=C(R)–CO–OH	-0.7(2) [55]	n.a.
CH$_2$=C(R)-CO-NH$_2$CH$_2$=C(R)–CO–NH$_2$	-6.5(6) [56]	4(2)

Conversely, the s-*trans* values obtained for the A and E states are significantly different from the predicted ones. A good agreement is obtained for the χ_{cc} component considering the average value between the A and E states:

$$\overline{\chi}_{gg} = \frac{\chi_{gg}^A + 2 \cdot \chi_{gg}^E}{3} \qquad g = a, b, c \tag{13}$$

that is $\overline{\chi}_{cc}$=-2.74(16) MHz against χ_{cc}^{MP2}=-2.75 MHz. Unfortunately, this approach does not work when applied to the χ_{aa} and χ_{bb} components. We note that the values of χ_{bb}^A and χ_{aa}^E are similar and that their average value $\overline{\chi}_{ba}^{AE}$=1.81(23) MHz is close to χ_{bb}^{MP2}=1.90 MHz. Although the values of χ_{aa}^A and χ_{bb}^E are not similar, again their average value $\overline{\chi}_{ab}^{AE}$=0.94(19) MHz is close to χ_{aa}^{MP2}=0.85 MHz. To sum up, a fair match between experimental and calculate values is achieved calculating the average values after exchanging the χ_{aa}^E and χ_{bb}^E values.

Stability

In Table 6 we compare the relative stability of the s-*trans* and s-*cis* conformers of methacrylamide with those of other acrolein derivatives. The s-*trans* conformer is more stable than the s-*cis* in the case of methacrylamide, methacryloil fluoride, and methacrylic acid, the latter two having a C$_s$ symmetry. The substitution of the methyl in the allyl group with a hydrogen atom results in a stabilization of the s-*cis* conformers. The stabilization energy is about 3–4 kJ mol^{-1}, except for methacrylamide where it is more than 10 kJ mol^{-1}.

Conclusions

The rotational spectrum recorded in the 59.4–104.0 GHz with a Stark modulated free-jet absorption millimeter wave spectrometer shows the presence of two forms of the molecule: the s-*trans* and the s-*cis*; the former one being the most stable one. The spectrum is characterized by a hyperfine structure related to the coupling of the nuclear quadrupole of the nitrogen nucleus to the overall rotation and to the torsion of the methyl group. Moreover, the signals of the s-*trans* form shows an additional splitting related to the inversion motion between two non-planar equivalent structures. Only a thorough analysis of the spectrum guided by high level quantum chemical calculations followed by an automatised flexible model, has allowed the correct description of the underlying nature of the motions involved. A fairly good match between the calculated and experimental quadrupole coupling constants of the s-*trans* conformer could only be achieved by calculating the average values after exchanging the χ_{aa} and χ_{bb} values. At the moment we are not able to explain this effect, and in order to confirm that it is not a simple numerical artifact, we are planning to study similar molecular systems. This study has provided structural information on both conformers of metacrylamide as well as an accurate determination of the barriers hindering the internal rotation and inversion motions and their dependence on the geometry.

Appendix
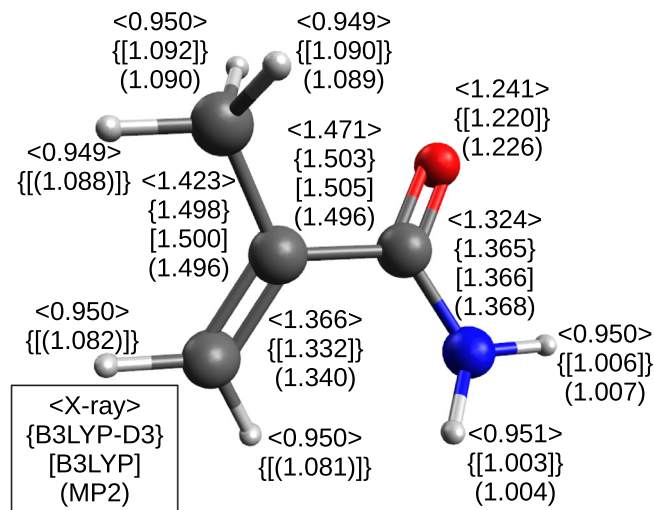
Fig. A1. Theoretical bond distances of isolated s-*trans*-methacrylamide calculated with the aug-cc-pVTZ basis set and X-ray solid state bond distances determined at 294 °C [41].

Table A1
Measured frequencies for s-*trans*-methacrylamide, ν [MHz].

$J''(K_a'',K_c'')-J'(K_a',K_c')$	$F''-F$	$\nu(A0^+)$	$\nu(A0^-)$	$\nu(E0^+)$	$\nu(E0^-)$	$\nu(A0^+-A0^-)$	$\nu(E0^+-E0^-)$	$\nu(A0^--A0^+)$	$\nu(E0^--E0^+)$
6(2,4)-5(1,5)	6-5	61542.21	61537.39	61541.70	61536.89				
6(2,4)-5(1,5)	7-6	61543.85	61539.00	61543.35	61538.55				
6(2,4)-5(1,5)	5-4	61544.21	61539.39	61543.35	61538.55				
6(6,0)-5(5,1)		60418.78	60418.10						
6(6,1)-5(5,0)		60414.92	60414.24						
6(6,0)-5(5,0)				60416.96	60416.21				
6(6,1)-5(5,1)				60416.21	60415.47				
6(6,0)-5(5,0)								61251.09	61252.49
6(6,1)-5(5,1)								61253.68	61251.68
7(3,4)-6(2,5)	7-6	65514.03	65508.92	65513.47	65508.42				
7(3,4)-6(2,5)	8-7	65515.22	65510.14	65514.70	65509.62				
7(3,4)-6(2,5)	6-5	65515.22	65510.14	65514.70	65509.62				
7(4,3)-6(3,4)	7-6	60077.03	60074.06	60076.53	60073.54				
7(4,3)-6(3,4)	8-7	60077.45	60074.48	60077.08	60074.06				
7(4,3)-6(3,4)	6-5	60077.45	60074.48	60077.08	60074.06				
7(5,2)-6(4,3)		61648.25	61645.49	61648.25	61645.49				
7(5,3)-6(4,2)		60740.84	60738.69	60740.49	60738.35				
7(6,1)-6(5,2)		66104.94	66104.10	66107.21	66106.31				
7(6,2)-6(5,1)		66064.44	66063.62	66061.69	66060.76				
7(7,0)-6(6,1)		70885.84	70885.05						
7(7,1)-6(6,0)		70885.05	70884.46						
7(6,1)-6(5,1)				66072.49	66071.66				
7(6,2)-6(5,2)				66096.23	66095.44				
7(7,0)-6(6,0)				70885.84	70885.05				
7(7,1)-6(6,1)				70884.46	70883.61				
7(5,2)-6(4,2)						60094.48	60094.48	61765.62	61765.45
7(5,3)-6(4,3)						60620.73	60620.37	62292.43	62292.07
7(6,1)-6(5,1)						65235.46	65236.95	66905.55	66907.04
7(6,2)-6(5,2)						65262.85	65260.71	66933.00	66930.88
7(7,0)-6(6,0)						70049.88	70050.36		71720.59
7(7,1)-6(6,1)						70050.36	70048.96		71719.20
8(3,5)-7(2,6)	8-7	78379.20	78372.71	78378.51	78372.05				
8(3,5)-7(2,6)	9-8	78380.45	78373.92	78379.76	78373.24				
8(3,5)-7(2,6)	7-6	78380.45	78373.92	78379.76	78373.24				
8(4,4)-7(3,5)	8-7	69849.98	69845.36	69849.48	69844.86				
8(4,4)-7(3,5)	9-8	69850.73	69846.09	69850.18	69845.55				
8(4,4)-7(3,5)	7-6	69850.73	69846.09	69850.18	69845.55				
8(5,3)-7(4,4)	9-8	68176.08	68178.37	68175.79	68178.07				
8(5,3)-7(4,4)	7-6	68176.08	68178.37	68175.79	68178.07				
8(5,4)-7(4,3)	9-8	65222.82	65226.94	65222.63	65226.74				
8(5,4)-7(4,3)	7-6	65222.82	65226.94	65222.63	65226.74				
8(6,2)-7(5,3)		71828.27	71827.23	71828.27	71827.23				
8(6,3)-7(5,2)		71594.36	71593.53	71593.53	71592.70				
8(7,1)-7(6,2)		76562.75	76561.82						
8(7,2)-7(6,1)		76554.93	76554.01						
8(8,0)-7(7,1)		81353.71	81352.72						
8(8,1)-7(7,0)		81353.71	81352.72						
8(7,1)-7(6,1)				76558.02	76558.02				
8(7,2)-7(6,2)				76558.76	76557.24				
8(8,0)-7(7,0)				81354.00	81353.08				
8(8,1)-7(7,1)				81352.72	81351.62				
8(1,7)-7(0,7)	8-7					63858.56	63858.18	65538.14	65537.77
8(1,7)-7(0,7)	9-8					63859.27	63858.89	65538.88	65538.48
8(1,7)-7(0,7)	7-6					63859.27	63858.89	65538.88	65538.48
8(2,6)-7(1,6)	8-7					62440.44	62439.90	64112.97	64112.40
8(2,6)-7(1,6)	9-8					62440.87	62440.44	64113.37	64112.97
8(2,6)-7(1,6)	7-6					62440.87	62440.44	64113.37	64112.97
8(2,7)-7(1,7)	8-7					63924.63	63924.26	65604.31	65603.92
8(2,7)-7(1,7)	9-8					63925.37	63924.96	65605.05	65604.64
8(2,7)-7(1,7)	7-6					63925.37	63924.96	65605.05	65604.64
8(3,6)-7(2,6)	8-7					63393.41	63392.91	65066.59	65066.12
8(3,6)-7(2,6)	9-8					63393.80	63393.41	65067.01	65066.59
8(3,6)-7(2,6)	7-6					63393.80	63393.41	65067.01	65066.59
8(3,5)-7(2,5)	8-7							61304.51	61304.15
8(3,5)-7(2,5)	9-8					59639.13	59638.73	61304.92	61304.51
8(3,5)-7(2,5)	7-6					59639.13	59638.73	61304.92	61304.51
8(4,4)-7(3,4)						59923.85	59923.55	61586.99	61586.69
8(4,5)-7(3,5)	8-7					63907.49	63907.16	65576.11	65575.81
8(4,5)-7(3,5)	9-8					63907.80	63907.49	65576.43	65576.11
8(4,5)-7(3,5)	7-6					63907.80	63907.49	65576.43	65576.11
8(5,3)-7(4,3)						65126.23	65125.99	66795.05	66794.78
8(5,4)-7(4,4)						66606.13	66605.82	68276.76	68276.49
8(6,2)-7(5,2)						70803.42	70803.42	72471.31	72471.31

J"(Ka",Kc")-J'(Ka',Kc')	F"-F	ν(A0⁺)	ν(A0⁻)	ν(E0⁺)	ν(E0⁻)	ν(A0⁺-A0⁻)	ν(E0⁺-E0⁻)	ν(A0⁻-A0⁺)	ν(E0⁻-E0⁺)
8(6,3)-7(5,3)						70950.20	70949.50	72618.28	72617.59
8(8,0)-7(7,0)								82187.60	82187.60
8(8,1)-7(7,1)								82187.60	82186.41
9(4,5)-8(3,6)	9-8	81503.03	81496.53	81502.22	81495.71				
9(4,5)-8(3,6)	10-9	81503.76	81497.25	81503.03	81496.53				
9(4,5)-8(3,6)	8-7	81503.76	81497.25	81503.03	81496.53				
9(5,4)-8(4,5)	9-8	75915.69	75912.01	75915.27	75911.60				
9(5,4)-8(4,5)	10-9	75916.13	75912.44	75915.69	75912.01				
9(5,4)-8(4,5)	8-7	75916.13	75912.44	75915.69	75912.01				
9(5,5)-8(4,4)		68636.04		68636.04	68636.04				
9(6,3)-8(5,4)		77725.17	77720.53	77725.17	77720.53				
9(6,4)-8(5,3)		76788.53	76784.67	76788.14	76784.31				
9(7,2)-8(6,3)		82232.28	82231.21	82234.51	82233.54				
9(7,3)-8(6,2)		82179.75	82178.75	82176.70	82175.71				
9(8,1)-8(7,2)		87030.68	87029.52						
9(8,2)-8(7,1)		87029.13	87028.11						
9(9,0)-8(8,1)		91821.52	91820.43						
9(9,1)-8(8,0)		91821.52	91820.43						
9(7,2)-8(6,2)				82190.19	82189.28				
9(7,3)-8(6,3)				82221.01	82220.00				
9(8,1)-8(7,1)				87030.14	87029.13				
9(8,2)-8(7,2)				87028.80	87027.75				
9(9,0)-8(8,0)				91821.52	91820.43				
9(9,1)-8(8,1)				91820.43	91819.21				
9(1,8)-8(0,8)	9-8					72071.83	72071.37	73753.60	73753.00
9(1,8)-8(0,8)	10-9					72072.44	72072.02	73754.10	73753.60
9(1,8)-8(0,8)	8-7					72072.44	72072.02	73754.10	73753.60
9(2,7)-8(1,7)	9-8					71012.33	71011.83	72686.03	72685.52
9(2,7)-8(1,7)	10-9					71012.80	71012.33	72686.50	72686.03
9(2,7)-8(1,7)	8-7					71012.80	71012.33	72686.50	72686.03
9(2,8)-8(1,8)	9-8					72093.68	72093.09	———	73774.78
9(2,8)-8(1,8)	10-9					72094.19	72093.68	73775.85	73775.39
9(2,8)-8(1,8)	8-7					72094.19	72093.68	73775.85	73775.39
9(3,6)-8(2,6)	9-8					68386.43	68386.00	70052.11	70051.65
9(3,6)-8(2,6)	10-9					68386.89	68386.43	70052.55	70052.11
9(3,6)-8(2,6)	8-7					68386.89	68386.43	70052.55	70052.11
9(3,7)-8(2,7)	9-8					71418.92	71418.42	73093.00	73092.50
9(3,7)-8(2,7)	10-9					71419.37	71418.92	73093.45	73093.00
9(3,7)-8(2,7)	8-7					71419.37	71418.92	73093.45	73093.00
9(4,5)-8(3,5)						66523.61	66523.27	68183.82	68183.45
9(4,6)-8(3,6)	9-8					71238.12	71237.79	72906.15	72905.80
9(4,6)-8(3,6)	10-9					71238.48	71238.12	72906.54	72906.15
9(4,6)-8(3,6)	8-7					71238.48	71238.12	72906.54	72906.15
9(5,5)-8(4,5)						72910.05	72909.70		
9(5,4)-8(4,4)						69977.81	69977.49	71638.15	71637.84
9(6,3)-8(5,3)						76153.14	76152.88		
10(4,6)-9(4,5)		61615.28	61613.77	61615.00	61613.50				
10(5,5)-9(5,4)		60748.82		60748.47	60745.98				
10(4,7)-9(3,6)	10-9	60222.30	60223.70	60222.30	60223.70				
10(4,7)-9(3,6)	11-10	60222.05	60223.47	60222.05	60223.47				
10(4,7)-9(3,6)	9-8	60222.05	60223.47	60222.05	60223.47				
10(5,5)-9(4,6)	10-9	85480.45	85474.83	85479.89	85474.27				
10(5,5)-9(4,6)	11-10	85481.04	85475.43	85480.45	85474.83				
10(5,5)-9(4,6)	9-8	85481.04	85475.43	85480.45	85474.83				
10(5,6)-9(4,5)	11-10	71038.97	71040.27	71038.97	71040.27				
10(5,6)-9(4,5)	9-8	71038.97	71040.27	71038.97	71040.27				
10(6,4)-9(5,5)			84129.52		84129.20				
10(6,5)-9(5,4)		81242.73	81247.53	81242.73	81247.53				
10(7,3)-9(6,4)		87925.56	87924.25	87925.56	87924.25				
10(7,4)-9(6,3)		87676.74	87675.71	87675.71	87674.68				
10(8,2)-9(7,3)		92693.44	92692.32						
10(8,3)-9(7,2)		92682.70	92681.55						
10(10,0)-9(9,1)		102288.97	102287.78						
10(10,1)-9(9,0)		102288.97	102287.78						
10(8,2)-9(7,2)				92686.68	92685.54				
10(8,3)-9(7,3)				92688.56	92687.44				
10(10,0)-9(9,0)				102288.97	102287.78				
10(10,1)-9(9,1)				102287.78	102286.59				
10(4,6)-9(3,6)	11-10					74226.70	74226.25		
10(4,6)-9(3,6)	9-8					74226.70	74226.25		
11(3,8)-10(3,7)		62098.04	62098.49	62098.04	62098.49				
11(4,7)-10(4,6)		66869.43	66868.61	66869.43	66868.61				
11(4,8)-10(4,7)		60965.43	60965.43	60965.43	60965.43				
11(5,6)-10(5,5)		67802.68	67800.03	67802.32	67799.70				

J"(K$_a$",K$_c$")-J'(K$_a$',K$_c$')	F"-F'	ν(A0⁺)	ν(A0⁻)	ν(E0⁺)	ν(E0⁻)	ν(A0⁺-A0⁻)	ν(E0⁺-E0⁻)	ν(A0⁻-A0⁺)	ν(E0⁻-E0⁺)
11(3,8)-10(4,7)		60053.99	60053.26	60053.99	60053.26				
11(4,8)-10(3,7)		63009.43	63010.65	63009.43	63010.65				
11(5,6)-10(4,7)		97073.40	97065.50	97072.68	97064.68				
11(5,7)-10(4,6)		72816.43	72818.38	72816.43	72818.38				
11(6,5)-10(5,6)		91631.37	91627.08	91630.85	91626.59				
11(6,6)-10(5,5)		84575.44	84575.44	84575.44	84575.44				
11(7,4)-10(6,5)		93760.55		93760.55					
11(7,5)-10(6,4)			92847.76		92847.24				
11(8,3)-10(7,4)		98340.76	98339.50	98343.24	98342.00				
11(8,4)-10(7,3)		98282.52	98281.33	98279.12	98277.89				
12(2,10)-11(2,9)		61790.79	61791.70	61790.79	61791.70				
12(3,10)-11(3,9)		61748.65	61749.51	61748.65	61749.51				
12(2,10)-11(3,9)		61727.24	61728.05	61727.24	61728.05				
12(3,9)-11(4,8)		65151.41	65151.41	65151.41	65151.41				
12(3,10)-11(2,9)		61812.19	61813.10	61812.19	61813.10				
12(4,8)-11(5,7)		65316.59	65313.84	65316.25	65313.48				
12(4,9)-11(3,8)		66431.48	66432.45	66431.48	66432.45				
12(5,8)-11(4,7)		74511.15	74513.29	74511.15	74513.29				
12(6,7)-11(5,6)	13-12	86734.56	86736.37	86734.56	86736.37				
12(6,7)-11(5,6)	11-10	86734.56	86736.37	86734.56	86736.37				
13(2,11)-12(2,10)			66108.57		66108.57				
13(3,11)-12(3,10)		66093.09	66094.13	66093.09	66094.13				
13(1,12)-12(2,11)		62237.80	62239.34	62237.80	62239.34				
13(2,11)-12(3,10)		66086.22	66087.26	66086.22	66087.26				
13(2,12)-12(1,11)		62238.60	62240.14	62238.60	62240.14				
13(3,10)-12(4,9)		69811.90	69811.90	69811.90	69811.90				
13(3,11)-12(2,10)		66114.52	66115.60	66114.52	66115.60				
13(4,9)-12(5,8)		71884.10	71882.51	71884.10	71882.51				
13(4,10)-12(3,9)		70319.63	70320.49	70319.63	70320.49				
13(5,9)-12(4,8)		76683.28	76685.13	76683.28	76685.13				
13(6,8)-12(5,7)		88082.20	88084.91	88082.20	88084.91				
14(0,14)-13(1,13)		62753.25	62755.49	62753.25	62755.49				
14(1,13)-13(2,12)		66581.85	66583.57	66581.85	66583.57				
14(1,14)-13(0,13)		62753.25	62755.49	62753.25	62755.49				
14(2,12)-13(3,11)		70430.92	70432.14	70430.92	70432.14				
14(2,13)-13(1,12)		66581.85	66583.57	66581.85	66583.57				
14(3,11)-13(4,10)		74268.95	74269.60	74268.95	74269.60				
14(3,12)-13(2,11)		70440.06	70441.28	70440.06	70441.28				
14(4,10)-13(5,9)		77397.27	77397.27	77397.27	77397.27				
14(4,11)-13(3,10)		74457.91	74458.82	74457.91	74458.82				
14(5,10)-13(4,9)		79617.47	79618.73	79617.47	79618.73				
14(6,9)-13(5,8)		89195.83	89198.81	89195.83	89198.81				
15(0,15)-14(1,14)		67098.24	67100.66	67098.24	67100.66				
15(1,14)-14(2,13)		70925.88	70927.78	70925.88	70927.78				
15(1,15)-14(0,14)		67098.24	67100.66	67098.24	67100.66				
15(2,13)-14(3,12)		74771.95	74773.37	74771.95	74773.37				
15(2,14)-14(1,13)		70925.88	70927.78	70925.88	70927.78				
15(3,12)-14(4,11)		78643.44	78644.28	78643.44	78644.28				
15(3,13)-14(2,12)		74774.78	74776.19	74774.78	74776.19				
15(4,11)-14(5,10)		82268.26	82268.26	82268.26	82268.26				
15(4,12)-14(3,11)		78710.45	78711.39	78710.45	78711.39				
15(5,11)-14(4,10)		83203.72	83204.61	83203.72	83204.61				
16(0,16)-15(1,15)		71443.15	71445.75	71443.15	71445.75				
16(1,15)-15(2,14)		75269.97	75272.07	75269.97	75272.07				
16(1,16)-15(0,15)		71443.15	71445.75	71443.15	71445.75				
16(2,14)-15(3,13)		79112.72	79114.22	79112.72	79114.22				
16(2,15)-15(1,14)		75269.97	75272.07	75269.97	75272.07				
16(3,13)-15(4,12)		82988.45	82989.53	82988.45	82989.53				
16(3,14)-15(2,13)		79113.57	79115.09	79113.57	79115.09				
16(4,12)-15(5,11)		86814.68	86814.68	86814.68	86814.68				
16(4,13)-15(3,12)		83011.32	83012.38	83011.32	83012.38				
16(5,12)-15(4,11)		87182.47	87183.32	87182.47	87183.32				
17(0,17)-16(1,16)		75787.93	75790.69	75787.93	75790.69				
17(1,16)-16(2,15)		79614.19	79616.47	79614.19	79616.47				
17(1,17)-16(0,16)		75787.93	75790.69	75787.93	75790.69				
17(2,15)-16(3,14)		83454.03	83455.76	83454.03	83455.76				
17(2,16)-16(1,15)		79614.19	79616.47	79614.19	79616.47				
17(3,14)-16(4,13)		87324.91	87326.13	87324.91	87326.13				
17(3,15)-16(2,14)		83454.03	83455.76	83454.03	83455.76				
17(4,14)-16(3,13)		87332.44	87333.68	87332.44	87333.68				
18(0,18)-17(1,17)		80132.51	80135.45	80132.51	80135.45				
18(1,17)-17(2,16)		83958.47	83960.89	83958.47	83960.89				
18(1,18)-17(0,17)		80132.51	80135.45	80132.51	80135.45				
18(2,16)-17(3,15)		87795.60	87797.51	87795.60	87797.51				

J"(K_a",K_c")-J'(K_a',K_c')	F"-F	ν(A0$^+$)	ν(A0$^-$)	ν(E0$^+$)	ν(E0$^-$)	ν(A0$^+$-A0$^-$)	ν(E0$^+$-E0$^-$)	ν(A0$^-$-A0$^+$)	ν(E0$^-$-E0$^+$)
18(2,17)-17(1,16)		83958.47	83960.89	83958.47	83960.89				
18(3,16)-17(2,15)		87795.60	87797.51	87795.60	87797.51				
19(0,19)-18(1,18)		84476.80	84480.00	84476.80	84480.00				
19(1,18)-18(2,17)		88302.45	88305.08	88302.45	88305.08				
19(1,19)-18(0,18)		84476.80	84480.00	84476.80	84480.00				
19(2,18)-18(1,17)		88302.45	88305.08	88302.45	88305.08				
20(0,20)-19(1,19)		88820.91	88824.33	88820.91	88824.33				
20(1,20)-19(0,19)		88820.91	88824.33	88820.91	88824.33				
21(0,21)-20(1,20)		93165.04	93168.66	93165.04	93168.66				
21(1,21)-20(0,20)		93165.04	93168.66	93165.04	93168.66				

Table A2
Measured frequencies for s-*cis*-methacrylamide, ν [MHz].

J"(K_a",K_c")-J'(K_a',K_c')	F"-F	ν(A)	ν(E)
5(4,2)-4(1,3)	5-4	60982.95	
5(4,2)-4(1,3)	6-5	60983.76	
5(4,2)-4(1,3)	4-3	60983.76	
6(4,3)-5(1,4)	6-5	68192.44	
6(4,3)-5(1,4)	7-6	68193.38	
6(4,3)-5(1,4)	5-4	68193.53	
6(2,4)-5(1,5)	6-5	64648.34	
6(2,4)-5(1,5)	7-6	64650.48	
6(2,4)-5(1,5)	5-4	64650.88	
6(3,4)-5(0,5)	6-5	67979.29	
6(3,4)-5(0,5)	7-6	67981.15	
6(3,4)-5(0,5)	5-4	67981.51	
6(4,3)-5(1,4)	6-5	68192.46	
6(4,3)-5(1,4)	7-6	68193.38	
6(4,3)-5(1,4)	5-4	68193.53	
6(6,1)-5(5,0)		60162.05	
6(6,0)-5(5,1)		60170.38	
6(6,0)-5(5,0)			60163.67
6(6,1)-5(5,1)			60168.82
7(3,4)-6(2,5)	7-6	69054.49	
7(3,4)-6(2,5)	8-7	69056.08	
7(3,4)-6(2,5)	6-5	69056.08	
7(4,3)-6(3,4)	7-6	61970.49	
7(4,3)-6(3,4)	8-7	61971.32	
7(4,3)-6(3,4)	6-5	61971.32	
7(5,3)-6(4,2)		60354.47	
7(5,2)-6(4,3)		61951.59	
7(6,2)-6(5,1)		65879.68	
7(6,1)-6(5,2)		65966.19	
7(7,0)-6(6,0)			70581.01
7(7,1)-6(6,1)			70581.45
8(4,4)-7(3,5)	8-7	73199.89	
8(4,4)-7(3,5)	9-8	73200.94	
8(4,4)-7(3,5)	7-6	73200.94	
8(5,4)-7(4,3)	8-7	64329.66	
8(5,4)-7(4,3)	9-8	64329.38	
8(5,4)-7(4,3)	7-6	64329.38	
8(5,3)-7(4,4)	7-6	69243.43	
8(5,3)-7(4,4)	9-8	69243.43	
8(6,3)-7(5,2)		71378.10	
8(6,2)-7(5,3)		71865.55	
8(7,2)-7(6,1)		76335.91	
8(7,1)-7(6,2)		76355.34	
8(8,1)-7(7,0)		80995.59	
8(8,0)-7(7,1)		80995.59	
9(5,4)-8(4,5)		78359.55	
9(5,5)-8(4,4)	9-8	67061.40	
9(5,5)-8(4,4)	10-9	67060.97	
9(5,5)-8(4,4)	8-7	67060.97	
9(6,4)-8(5,3)		76274.53	
9(6,3)-8(5,4)		78154.37	
9(7,3)-8(6,2)		82009.08	
9(7,2)-8(6,3)		82137.93	
9(8,2)-8(7,1)		86762.00	
9(8,1)-8(7,2)		86766.29	
9(9,1)-8(8,0)		91409.55	
9(9,0)-8(8,1)		91409.55	
9(8,1)-8(7,1)			86763.05
9(8,2)-8(7,2)			86765.26

(*continued on next page*)

Table A2 (*continued*)

J''(K_a'',K_c'')–J'(K_a',K_c')	F''–F'	ν(A)	ν(E)
10(4,6)-9(4,5)		62458.22	
10(5,5)-9(5,4)		62911.79	
10(6,4)-9(6,3)		60346.80	
10(5,6)-9(4,5)	10-9	68873.64	
10(5,6)-9(4,5)	11-10	68873.18	
10(5,6)-9(4,5)	9-8	68873.18	
10(6,5)-9(5,4)	10-9	80036.14	
10(6,5)-9(5,4)	11-10	80035.97	
10(6,5)-9(5,4)	9-8	80035.97	
10(6,4)-9(5,5)	10-9	85439.75	
10(6,4)-9(5,5)	11-10	85439.89	
10(6,4)-9(5,5)	9-8	85439.89	
10(7,4)-9(6,3)		87429.13	
10(7,3)-9(6,4)		88022.61	
10(8,3)-9(7,2)		92492.41	
10(8,2)-9(7,3)		92523.42	
11(5,7)-10(5,6)		63954.54	
11(3,8)-10(3,7)		61442.76	
11(4,8)-10(4,7)		60799.70	
11(4,7)-10(4,6)		66950.38	
11(6,5)-10(6,4)		67817.88	
11(7,4)-10(7,3)		65521.18	
11(7,5)-10(7,4)		65132.71	
11(3,8)-10(4,7)		60407.19	
11(4,8)-10(3,7)		61835.22	
11(4,7)-10(5,6)		60535.33	
11(5,7)-10(4,6)	11-10	70369.92	
11(5,7)-10(4,6)	12-11	70369.49	
11(5,7)-10(4,6)	10-9	70369.49	
11(6,6)-10(5,5)	11-10	82421.84	
11(6,6)-10(5,5)	12-11	82421.51	
11(6,6)-10(5,5)	10-9	82421.51	
11(7,5)-10(6,4)		92214.86	
12(2,10)-11(2,9)		61027.93	
12(3,10)-11(3,9)		61012.10	
12(3,9)-11(3,8)		65394.75	
12(4,9)-11(4,8)		65138.89	
12(4,8)-11(4,7)		70700.09	
12(5,8)-11(5,7)		68831.92	
12(5,7)-11(5,6)		75494.96	
12(6,6)-11(6,5)		75462.17	
12(2,10)-11(3,9)		61005.54	
12(3,10)-11(2,9)		61034.55	
12(3,9)-11(4,8)		65002.38	
12(4,9)-11(3,8)		65531.27	
12(4,8)-11(5,7)		67280.93	
12(5,8)-11(4,7)	12-11	72251.37	
12(5,8)-11(4,7)	13-12	72251.00	
12(5,8)-11(4,7)	11-10	72251.00	
12(5,7)-11(6,6)		62799.55	
13(2,11)-12(2,10)		65237.91	
13(3,11)-12(3,10)		65233.16	
13(3,10)-12(3,9)		69486.45	
13(5,8)-12(5,7)		80087.44	
13(1,12)-12(2,11)		61105.24	
13(2,12)-12(1,11)		61105.24	
13(2,11)-12(3,10)		65231.26	
13(3,11)-12(2,10)		65239.75	
13(4,10)-12(3,9)		69531.00	
13(5,9)-12(4,8)		74952.45	
13(6,8)-12(6,7)		76424.90	
13(6,7)-12(6,6)		82541.71	
13(7,7)-12(7,6)		77566.44	
14(2,12)-13(2,11)		69455.01	
14(3,12)-13(3,11)		69453.62	
14(4,11)-13(4,10)		73617.65	
14(4,10)-13(4,9)		78162.63	
14(0,14)-13(1,13)		61226.36	
14(1,14)-13(0,13)		61226.36	
14(1,13)-13(2,12)		65330.56	

Table A2 (*continued*)

J''(K_a'',K_c'')-J'(K_a',K_c')	F''-F	ν(A)	ν(E)
14(2,13)-13(1,12)		65330.56	
14(2,12)-13(3,11)		69453.13	
14(3,12)-13(2,11)		69455.50	
14(3,11)-13(4,10)		73603.77	
14(3,11)-13(3,10)		73648.31	
14(4,11)-13(3,10)		73662.15	
14(4,10)-13(5,9)		77541.46	
15(4,12)-14(4,11)		77831.50	
15(3,12)-14(3,11)		77841.17	
15(0,15)-14(1,14)		65452.94	
15(1,15)-14(0,14)		65452.94	
15(1,14)-14(2,13)		69556.17	
15(2,14)-14(1,13)		69556.17	
15(2,13)-14(3,12)		73674.80	
15(3,13)-14(2,12)		73675.35	
15(3,12)-14(4,11)		77827.32	
15(4,12)-14(3,11)		77845.30	
15(5,11)-14(4,10)		82258.64	
16(0,16)-15(1,15)		69679.49	
16(1,16)-15(0,15)		69679.49	
16(1,15)-15(2,14)		73781.82	
16(2,15)-15(1,14)		73781.82	
16(2,14)-15(3,13)		77897.24	
16(3,14)-15(2,13)		77897.24	
16(3,13)-15(4,12)		82043.53	
16(4,13)-15(3,12)		82048.89	
17(0,17)-16(1,16)		73906.08	
17(1,17)-16(0,16)		73906.08	
17(1,16)-16(2,15)		78007.75	
17(2,16)-16(1,15)		78007.75	
17(2,15)-16(3,14)		82120.41	
17(3,15)-16(2,14)		82120.41	
18(0,18)-17(1,17)		78132.49	
18(1,18)-17(0,17)		78132.49	
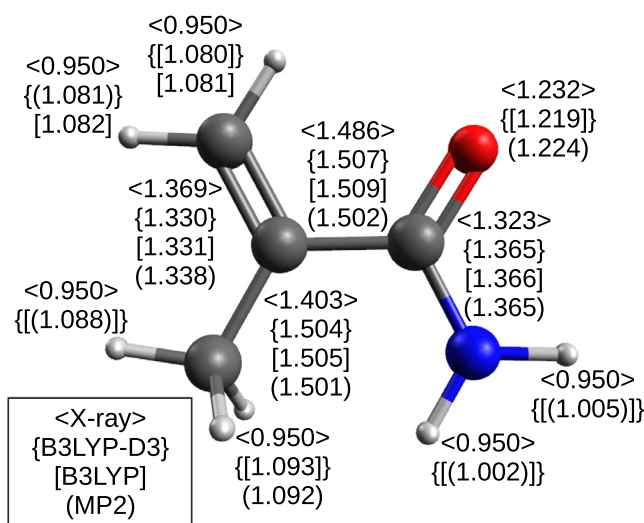
Fig. A2. Theoretical bond distances of isolated *s-cis*-methacrylamide calculated with the aug-cc-pVTZ basis set and X-ray solid state bond distances determined at 294 °C [41].

References

[1] C.P. Endres, S. Schlemmer, P. Schilke, J. Stutzki, H.S.P. Müller, J. Mol. Spectrosc. 327 (2016) 95–104, doi:10.1016/j.jms.2016.03.005.

[2] S. Melandri, L. Evangelisti, S. Canola, H. Sa'adeh, C. Calabrese, M. Coreno, C. Grazioli, K.C. Prince, F. Negri, A. Maris, Phys. Chem. Chem. Phys. 22 (2020) 13440–13455, doi:10.1039/D0CP02304C.

[3] A. Maris, C. Calabrese, L.B. Favero, L. Evangelisti, I. Usabiaga, S. Mariotti, C. Codella, L. Podio, N. Balucani, C. Ceccarelli, B.L. Lefloch, S. Melandri, Earth Space Chem. 3 (2019) 1537–1549, doi:10.1021/acsearthspacechem.9b00084.

[4] I. Usabiaga, A. Camiruaga, C. Calabrese, A. Maris, J.A. Fernández, Chem. Eur. J. 25 (2019) 14230–14236, doi:10.1002/chem.201903478.

[5] A. Vigorito, L. Paoloni, C. Calabrese, L. Evangelisti, L.B. Favero, S. Melandri, A. Maris, J. Mol. Spectrosc. 342 (2017) 38–44, doi:10.1016/j.jms.2017.04.014.

[6] C. Calabrese, A. Maris, I. Uriarte, E.J. Cocinero, S. Melandri, Chem. Eur. J. 23 (2017) 3595–3604, doi:10.1002/chem.201604891.

[7] A. Maris, Phys. Chem. Chem. Phys. 6 (2004) 2611–2616, doi:10.1039/B401081G.

[8] A. Maris, S. Melandri, W. Caminati, P.G. Favero, Chem. Phys. 283 (2002) 111–118, doi:10.1016/S0301-0104(02)00499-8.

[9] P. Ottaviani, S. Melandri, A. Maris, P.G. Favero, W. Caminati, J. Mol. Spectrosc. 205 (2001) 173–176, doi:10.1006/jmsp.2000.8243.

[10] W. Caminati, A. Maris, A. Millemaggi, New J. Chem. 24 (2000) 821–824, doi:10.1039/B005410K.

[11] R. Fernandes, P. Amador, C. Prudêncio, Rev. Med. Microbiol. 24 (2013) 7–17, doi:10.1097/MRM.0b013e3283587727.

[12] S. Suzuki, P. Gerner, P. Lirk, 20-Local anesthetics, in: H.C. Hemmings, T.D. Egan (Eds.), Pharmacology and physiology for anesthesia (second edition), Elsevier, Philadelphia, 2019, pp. 390–411, doi:10.1016/B978-0-323-48110-6.00020-X.

[13] C.V. Sharma, V. Mehta, CEACCP 14 (2014) 153–158, doi:10.1093/bjaceaccp/mkt049.

[14] J.C. Kendrew, G. Bodo, H.M. Dintzis, R.G. Parrish, H. Wyckoff, D.C. Phillips, Nature 181 (1958) 662–666, doi:10.1038/181662a0.

[15] C.C.F. Blake, D.F. Koenig, G.A. Mair, A.C.T. North, D.C. Phillips, V.R. Sarma, Nature 206 (1965) 757–761, doi:10.1038/206757a0.

[16] H.M. Badawi, M.A.A. Al-Khaldi, S.S.A. Al-Abbad, Z.H.A. Al-Sunaidi, Spectrochim. Acta A 68 (2007) 432–442, doi:10.1016/j.saa.2006.11.048.

[17] T. Jr. Dunning, J. Chem. Phys. 90 (1989) 1007–1023, doi:10.1063/1.456153.

[18] C. Møller, M. Plesset, Phys. Rev. 46 (1934) 618–622, doi:10.1103/PhysRev.46.618.

[19] A. Becke, J. Chem. Phys. 98 (1993) 5648–5652, doi:10.1063/1.464913.

[20] C. Lee, W. Yang, R. Parr, Phys. Rev. B 37 (1988) 785–789, doi:10.1103/PhysRevB.37.785.

[21] S. Grimme, J. Antony, S. Ehrlich, H. Krieg, J. Chem. Phys. 132 (2010) 154104, doi:10.1063/1.3382344.

[22] V. Barone, J. Chem. Phys. 122 (2005) 014108, doi:10.1063/1.1824881.

[23] L. Paoloni, A. Maris, J. Phys. Chem. A 125 (2021) 4098–4113, doi:10.1021/acs.jpca.1c01472.

[24] C. Calabrese, A. Vigorito, A. Maris, S. Mariotti, P. Fathi, W.D. Geppert, S. Melandri, J. Phys. Chem. A 119 (2015) 11674–11682, doi:10.1021/acs.jpca.5b08426.

[25] A. Vigorito, C. Calabrese, S. Melandri, A. Caracciolo, S. Mariotti, A. Giannetti, M. Massardi, A. Maris, A&A 619 (2018) A140, doi:10.1051/0004-6361/201833489.

[26] S. Melandri, P.G. Favero, D. Damiani, W. Caminati, L.B. Favero, J. Chem. Soc. Faraday Trans. 90 (1994) 2183–2188, doi:10.1039/FT9949002183.

[27] H.M. Pickett, J. Mol. Spectrosc. 148 (1991) 371–377, doi:10.1016/0022-2852(91)90393-O.

[28] J. Watson, Vibrational Spectra and Structure, Elsevier, New York/Amsterdam, 1977.

[29] C.C. Lin, J.D. Swalen, Rev. Mod. Phys. 31 (1959) 841–892, doi:10.1103/RevModPhys.31.841.

[30] B. Ouyang, B.J. Howard, Phys. Chem. Chem. Phys. 11 (2009) 366–373, doi:10.1039/B814562H.

[31] H.M. Pickett, J. Chem. Phys. 56 (1972) 1715–1723, doi:10.1063/1.1677430.

[32] H.S.P. Müller, A. Belloche, L.-H. Xu, R.M. Lees, R.T. Garrod, A. Walters, J. van Wijngaarden, F. Lewen, S. Schlemmer, K.M. Menten, A&A 587 (2016) A92, doi:10.1051/0004-6361/201527470.

[33] J.C. Pearson, B.J. Drouin, J. Mol. Spectrosc. 234 (2005) 149–156, doi:10.1016/j.jms.2005.08.013.

[34] F. Scappini, H. Dreizler, Z. Naturforsch. A 36 (1981) 1327–1333, doi:10.1515/zna-1981-1210.

[35] Woods, R. (1966). J. Mol. Spectrosc., 21, 4–24. 10.1016/0022-2852(66)90117-2

[36] H. Hartwig, H. Dreizler, Z. Naturforsch. 51a (1996) 923–932, doi:10.1515/zna-1996-0807.

[37] Oka, T. (1995). J. Mol. Struct., 352/353 (1995) 225-233, doi:10.1016/0022-2860(95)08844-L

[38] C.C. Costain, J.M. Dowling, J. Chem. Phys. 32 (1960) 158–165, doi:10.1063/1.1700891.

[39] E. Hirota, R. Sugisaki, C.J. Nielsen, G.O. Sørensen, J. Mol. Spectrosc. 49 (1974) 251–267, doi:10.1016/0022-2852(74)90274-4.

[40] J. Demaison, A. G. Császár, I. Kleiner, H. Møllendal, J. Phys. Chem. A 111 (2007) 2574–2586, doi:10.1021/jp067278j.

[41] C. Guo, M.B. Hickey, E.R. Guggenheim, V. Enkelmann, B.M. Foxman, Chem. Commun. (2005) 2220–2222, doi:10.1039/B418869A.

[42] D.J. Herschbach, J. Chem. Phys. 31 (1959) 91–108, doi:10.1063/1.1730343.

[43] D.J. Herschbach, J. Chem. Phys. 27 (1957), doi:10.1063/1.1743897. 975–975

[44] W. Gordy, R. Cook, Microwave Molecular Spectra, Wiley, New York, 1984.

[45] S. Herbers, P. Kraus, J.-U. Grabow, J. Chem. Phys. 150 (2019) 144308/1–10, doi:10.1063/1.5091693.

[46] J. Durig, J. Qiu, B. Dehoff, T. Little, Spectroch. Acta 42A (1986) 89–103, doi:10.1016/0584-8539(86)80168-4.

[47] O. Zakharenko, R. Motiyenko, J.-R.A. Moreno, A. Jabri, I. Kleiner, T.R. Huet, J. Chem. Phys. 144 (2015) 024303/1–9, doi:10.1063/1.4939636.

[48] R.G. Latypova, A.K. Mamleev, L.N. Gunderova, N.M. Pozdeev, J. Struct. Chem. 17 (1976) 728–731, doi:10.1007/BF00746013.

[49] S. Blanco, J.C. López, A. Lesarri, J.L. Alonso, J. Am. Chem. Soc. 128 (2006) 12111–12121, doi:10.1021/ja0618393.

[50] R.D. Suenram, G.Y. Golubiatnikov, I.I. Leonov, J.T. Hougen, J. Ortigoso, I. Kleiner, G.T. Fraser, J. Mol. Spectros. 208 (2001) 188–193, doi:10.1006/jmsp.2001.8377.

[51] E.R. Alonso, L. Kolesniková, A. Belloche, S. Mata, R.T. Garrod, A. Jabri, I. Le 'on, J.-C. Guillemin, H.S.P. Müller, K.M. Menten, J.L. Alonso, A&A 647 (2021) A55, doi:10.1051/0004-6361/202040211.

[52] A.C.P. Alves, J. Christoffersen, J.M. Hollas, Mol. Phys. 20 (1971) 625–644, doi:10.1080/00268977100100601.

[53] J.J. Keirns, R.F. Curl, J. Chem. Phys. 48 (1968) 3773–3778, doi:10.1063/1.1669684.

[54] R. Latypova, L. Gunderova, A. Mamleev, N. Pozdeev, J. Struct. Chem. 21 (1980) 315–320, doi:10.1007/BF00746851.

[55] K. Bolton, D. Lister, J. Sheridan, J. Chem. Soc. Faraday Trans. 70 (1974) 113–123, doi:10.1039/F29747000113.

[56] K.-M. Marstokk, H. Møllendal, S. Samdal, J. Mol. Struct. 524 (2000) 69–85, doi:10.1016/S0022-2860(99)00362-2.